

On Sampling Errors in Empirical Orthogonal Functions

ROBERTA QUADRELLI, CHRISTOPHER S. BRETHERTON, AND JOHN M. WALLACE

University of Washington, Seattle, Washington

(Manuscript received 6 February 2004, in final form 7 March 2005)

ABSTRACT

A perturbation analysis is carried out to quantify the eigenvector errors due to the mixing with other eigenvectors that occur when empirical orthogonal functions (EOFs) are computed for a finite-size data sample. Explicit forms are provided for the second-order eigenvalue error and first-order eigenvector error. The eigenvector sampling error depends monotonically on the ratio of the lower to the higher eigenvalues that mix. The relationship to the eigenvalue separation criterion of North et al. is discussed.

The eigenvector error formula is applied to quantify sampling errors for the leading EOF of the Northern Hemisphere wintertime geopotential height at various pressure levels, and it is found that the smallest sampling error in the troposphere occurs for the sea level pressure EOF. The errors in the 500-hPa height EOFs are almost twice as large.

1. Introduction

It is known that the eigenvalues and empirical orthogonal functions (EOFs) for a finite sample are only estimates of the “true” eigenvalues and eigenvectors that would be perfectly recovered from an infinite size dataset.

North et al. (1982) derived an explicit form for the first-order errors in the eigenvalues λ_i of the covariance matrix for a sample of T independent realizations in time. The resulting formula,

$$\delta\lambda_i \approx 2^{1/2}\varepsilon\lambda_i, \quad (1)$$

where $\varepsilon = T^{-1/2}$, has been extensively used to estimate the sampling variability. Eigenvalues with overlapping errors can be regarded as “effective multiplets”; one should avoid truncating an EOF decomposition within such a range. North et al. (1982) do not provide an explicit estimate for the error associated with eigenvectors; their Eq. (23) also relies on a hypothetical form of the sample covariance matrix.

Several other papers in meteorology have dealt with

the sampling variability issue. The statistical properties of estimated eigenvalues and eigenvectors for small samples have been studied (Storch and Hannoschöck 1985), and bounds for sampling variability errors have been proposed (Kim 1996). The same issue has been widely studied in the statistical literature, as discussed in chapter 4 of Jackson (1991), starting with Girshick (1939), who derived the form of asymptotic errors in eigenvectors, but it has not been sufficiently exploited in climate statistics studies.

It is important for a number of geophysical applications to be able to quantify uncertainties not only in the eigenvalues, but also in the eigenvectors. Examples include assessing whether a pattern that resembles the leading EOF should be interpreted as a realization of that EOF or as a distinctly different pattern (Quadrelli and Wallace 2004), and determining whether the leading EOFs derived from two different datasets (either observations or model output) are distinctly different from one another.

Here we quantify the uncertainties in EOFs estimated from a finite data sample. We propose a general formula that complements the formula for the degree of separation between eigenvalues given in North et al. (1982) and enables a more thorough analysis on eigenvector errors.

This note is comprised of five parts. In the next section we derive an analytical expression for the errors

Corresponding author address: Roberta Quadrelli, JISAO, Dept. of Atmospheric Sciences, University of Washington, Box 354235, Seattle, WA 98195-4235.
E-mail: roberta@atmos.washington.edu

(to first order for eigenvectors and second order for eigenvalues) in sample EOF estimates. In section 3 mixing errors in the leading EOF are analyzed for a hypothetical dataset with a prescribed eigenvalue spectrum. In section 4 the results are applied to the observed Northern Hemisphere geopotential height field. Sampling errors for the leading EOF at several height levels are compared, and it is deduced that mode mixing is smaller at the earth's surface than in the midtroposphere. Conclusions are given in section 5.

2. Eigenvalue and eigenvector sampling errors

The magnitude of the sampling error associated with a single eigenvector depends on how much it tends to mix with each of the other eigenvectors of the sample. Any eigenvector $\hat{\mathbf{e}}$ of a finite size dataset is generally located at an angle α from the direction of the true corresponding eigenvector \mathbf{e} , and the sampling error \mathbf{e}' can be expressed as a linear combination of all the other true eigenvectors \mathbf{e}_i . In this paper we will find that if the eigenvalues are well separated, the typical size of α will be $O(\epsilon)$, and, to first order in ϵ , \mathbf{e}' is orthogonal to \mathbf{e} .

We consider the case of a dataset with T independent realizations in time over N grid points, where the grid spacing is dense enough that spatial sampling errors are not important. In general the number of resulting EOFs is $N^* = \min(T - 1, N)$.

The mathematical formulation of the sampling problem is based on appendix A of Bretherton et al. (1999), part b. Here we follow their approach of working in the basis of the true eigenvectors, which are obtained from the true covariance matrix \mathbf{C} . If \mathbf{E} is the orthogonal matrix whose columns are the normalized eigenvectors, and $\mathbf{\Lambda}$ is the diagonal matrix of the eigenvalues λ_i , then

$$\mathbf{\Lambda} = \mathbf{E}^T \mathbf{C} \mathbf{E}. \quad (2)$$

With only T independent realizations in time, none of the elements of $\mathbf{\Lambda}$, \mathbf{E} , and \mathbf{C} are known precisely. The corresponding variables obtained directly from the finite data sample will be denoted by ($\hat{\cdot}$).

Applying the transformation of (2) to $\hat{\mathbf{C}}$ (instead of \mathbf{C}), we obtain a new matrix, $\hat{\mathbf{L}}$:

$$\hat{\mathbf{L}} = \mathbf{E}^T \hat{\mathbf{C}} \mathbf{E}.$$

The eigenvectors of $\hat{\mathbf{L}}$ correspond to the eigenvectors of $\hat{\mathbf{C}}$, but they are expressed in the basis of the true

eigenvectors \mathbf{e}_i . In fact the eigenvalue equations for $\hat{\mathbf{L}}$ and $\hat{\mathbf{C}}$ are related by the fact that if

$$\hat{\mathbf{L}} \hat{\mathbf{e}} = \hat{\lambda} \hat{\mathbf{e}}, \quad (3)$$

then $\hat{\mathbf{C}} \hat{\mathbf{y}} = \hat{\lambda} \hat{\mathbf{y}}$, with $\hat{\mathbf{y}} = \mathbf{E} \hat{\mathbf{e}}$, and $\|\hat{\mathbf{y}}_i - \hat{\mathbf{y}}_j\| = \|\hat{\mathbf{e}}_i - \hat{\mathbf{e}}_j\|$ from the properties of the orthogonal matrix \mathbf{E} .

Therefore the sampling problem for the eigenvectors of $\hat{\mathbf{C}}$ can be solved by working in the basis of the \mathbf{e}_i and defining the errors as departures of the eigenvectors $\hat{\mathbf{e}}_i$ of $\hat{\mathbf{L}}$ from the corresponding true eigenvectors \mathbf{e}_i . Since $\hat{\mathbf{L}}$ is symmetric and positive definite, it has real, orthonormal eigenvectors. It can be interpreted as a perturbed form $\hat{\mathbf{L}} = (\mathbf{\Lambda} + \epsilon \mathbf{P})$ of the diagonal matrix $\mathbf{\Lambda}$. Bretherton et al. (1999) showed that for a large number of independent samples (T), the elements of \mathbf{P} can be expressed in terms of T , the true eigenvalues λ_i , and uncorrelated unit normal random perturbations (w_{ij}):

$$\mathbf{P}_{ij} = \begin{cases} 2^{1/2} \lambda_j w_{ii} & j = i \\ \lambda_i^{1/2} \lambda_j^{1/2} w_{ij} & j \neq i \end{cases}, \quad (4)$$

where

$$\epsilon = T^{-1/2} \ll 1. \quad (5)$$

For an infinite sample length, $\hat{\mathbf{L}} \rightarrow \mathbf{\Lambda}$ (and no mode mixing occurs).

The eigenvalues $\hat{\lambda}_i$ and eigenvectors $\hat{\mathbf{e}}_i$ of (3) can be expressed as perturbation series:

$$\hat{\lambda}_i = \lambda_i + \kappa_{i1} \epsilon + \kappa_{i2} \epsilon^2 \dots, \quad (6)$$

$$\hat{\mathbf{e}}_i = \mathbf{e}_i + \epsilon \hat{\mathbf{e}}_{i1} + \epsilon^2 \hat{\mathbf{e}}_{i2} \dots \quad (7)$$

The solution of this perturbation problem (i.e., the terms k_{ij} and $\hat{\mathbf{e}}_{ij}$) can be found in the statistics literature. Wilkinson (1965) showed that the first-order perturbation to the i th eigenvector is a sum of independent perturbations deriving from the mixing occurring between that eigenvector and each of the other $N - 1$ eigenvectors:

$$\hat{\mathbf{e}}_{i1} = \sum_{j \neq i} \frac{\mathbf{P}_{ij} \mathbf{e}_j}{(\lambda_i - \lambda_j)}. \quad (8)$$

Recalling the expression (4) for \mathbf{P}_{ij} , this implies that the perturbed eigenvectors have the form

$$\hat{\mathbf{e}}_i = \mathbf{e}_i + \sum_{j \neq i} \alpha_{ij} \mathbf{e}_j + O(\epsilon^2), \quad (9)$$

where

$$\alpha_{ij} = \alpha_{ij}^* w_{ij}, \quad (10)$$

$$\alpha_{ij}^* = \epsilon \frac{\beta_{ij}^{1/2}}{(1 - \beta_{ij})}, \quad (11)$$

$$\beta_{ij} = \frac{\lambda_j}{\lambda_i}. \quad (12)$$

The absolute value of α_{ij}^* corresponds to the standard deviation of α_{ij} because the w_{ij} are unit random perturbations. Note that the perturbation theory is valid only if $|\alpha_{ij}^*| \ll 1$.

Wilkinson also showed that, to second order in ϵ ,

$$\hat{\lambda}_i = \lambda_i(1 + \sqrt{2}\epsilon w_{ii}) + \epsilon^2 \sum_{j \neq i} \frac{\lambda_j}{(1 - \beta_{ij})} w_{ij}^2. \quad (13)$$

To first order, (13) is consistent with the criterion of North et al. (1982) referred to here in (1). In that same paper, it is noted that the first-order perturbation for a given *eigenvalue* is independent of its spacing with respect to other eigenvalues. In contrast, it is clear from (11) that the first-order *eigenvector* perturbation is strongly dependent on the ratio of the mixing eigenvalues.

Also, while the first-order shift of the eigenvalues has random sign, the second-order bias is positive or negative depending on the relative ranking of the two eigenvalues that mix. Consistent with previous observations of Storch and Hannochöck (1985), the largest eigenvalues tend to be overestimated and the smallest ones underestimated.

The two key factors that determine the typical mixing between pairs of eigenvectors i, j are thus as follows:

- the ratio β_{ij} between the corresponding eigenvalues (the closer the ratio to 1, the larger the error), and
- the number T of independent realizations in time.

For geophysical data, the number of independent realizations in time T is generally smaller than the actual sample size, because of serial time dependence. Therefore, an estimate of the effective number of degrees of freedom T^* should be computed from the sample (as done in the example of section 4).

Figure 1 shows the dependence of the individual error contribution α_{ij}^* (representing mixing of eigenvectors i and j only) upon the eigenvalue ratio $\beta_{ij} = \lambda_j/\lambda_i$ and the sample size T . Within the range represented (for small values of α_{ij}), the perturbation theory is valid, and $\arctan(\alpha_{ij}) \approx \alpha_{ij}$; thus, α_{ij} represents the angular error in the plane i, j , and α_{ij}^* is its standard deviation. Only ratios β_{ij} smaller than 1 (i.e., mixing with eigenvectors of lower order) are plotted, since the absolute value of α_{ij}^* is the same for a ratio β_{ij} and for its reciprocal. This is because the mixing between eigenvectors i and j contributes equally to errors in $\hat{\mathbf{e}}_i$ (for which $\beta_{ij} = \lambda_j/\lambda_i$) and $\hat{\mathbf{e}}_j$.

The total error is a sum of contributions from each direction; an estimate of the overall accuracy in the computation of an eigenvector \mathbf{e}_i is the expected spatial correlation coefficient between a random sample real-

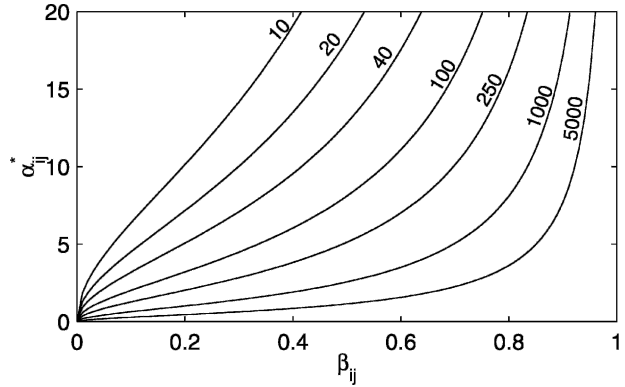


FIG. 1. Standard deviation of the error angle α_{ij} ($^\circ$) due to mixing between eigenvectors i and j , vs ratio $\beta_{ij} = \lambda_j/\lambda_i$, as in (11), for 10, 20, 40, 100, 250, 1000, and 5000 independent realizations in time (T), as indicated.

ization $\hat{\mathbf{e}}_i$ and \mathbf{e}_i : $r = E[\hat{\mathbf{e}}_i \cdot \mathbf{e}_i]$, where E denotes an expected value. Note that $\hat{\mathbf{e}}_i$ is given by (9) to $O(\epsilon)$, but for this calculation it must be normalized back to a unit vector [an $O(\epsilon^2)$ correction]. Hence, to first order,

$$r = E \left[\frac{\mathbf{e}_i + \sum_{j \neq i} \alpha_{ij} \mathbf{e}_j}{(1 + \sum_{j \neq i} \alpha_{ij}^2)^{1/2}} \cdot \mathbf{e}_i \right] \quad (14)$$

$$= E \left[\frac{1}{(1 + \sum_{j \neq i} \alpha_{ij}^2)^{1/2}} \right] \quad (15)$$

$$= E \left[1 - 0.5 \sum_{j \neq i} \alpha_{ij}^2 \right] \quad (16)$$

$$= 1 - 0.5 \sum_{j \neq i} \alpha_{ij}^{*2}. \quad (17)$$

The third step above follows since the α_{ij}^* are assumed small for large T , or else the perturbation theory is not accurate. The last step follows since $E(\alpha_{ij}^2) = \alpha_{ij}^{*2}$.

We now show that if the North et al. eigenvalue separation criterion is satisfied for the leading eigenvalue λ_1 , then the sample EOF1 is expected to be well correlated with the true EOF1. For the leading eigenvector, the North et al. (1982) separation criterion is satisfied when

$$\lambda_1 - \lambda_2 \geq \delta\lambda_1 + \delta\lambda_2 \approx (\lambda_1 + \lambda_2)\sqrt{2}\epsilon, \quad (18)$$

or, since $\epsilon \ll 1$,

$$\beta_{12} = \frac{\lambda_2}{\lambda_1} < \beta_c = 1 - 2\sqrt{2}\epsilon. \quad (19)$$

If the remaining eigenvalues are well separated from λ_1 , they will contribute only $O(\epsilon^2)$ to the correlation r . Neglecting these contributions to (17),

$$r = 1 - 0.5\alpha_{12}^{*2} \quad (20)$$

$$= 1 - 0.5\epsilon^2 \frac{\beta_{12}}{(1 - \beta_{12})^2} \quad (21)$$

$$> 1 - 0.5\epsilon^2 \frac{\beta_c}{(1 - \beta_c)^2} = 1 - \frac{1}{16} + \frac{\sqrt{2}}{8}\epsilon = 0.9375. \quad (22)$$

The formula given in (22) can be trivially generalized to eigenvectors of any order. Also, from (17) it is clear that EOFs of order higher than 1 tend to be subject to greater uncertainty than the leading EOF, even if their eigenvalues are just as well separated from their nearest neighbors as λ_1 is separated from λ_2 . This is because of the cumulative effects of mixing with other nearby EOFs of both higher and lower order.

3. Mixing error in the leading EOF: An example

In this section we estimate the sample size needed in order to obtain acceptably small errors in the computation of the leading EOF. We consider a hypothetical multivariate random process whose true covariance matrix has N eigenvalues, chosen as follows. It is assumed that $\beta_{12} = \lambda_2/\lambda_1$ can take any possible value $0 < \beta_{12} < 1$, that the eigenvalues from the third onward decrease exponentially with a constant ratio $\beta = \lambda_{j+1}/\lambda_j$, and that the N eigenvalues sum to 1. This uniquely defines all the eigenvalues as follows:

$$\begin{cases} \lambda_1 = \left(1 + \beta_{12} \frac{1 - \beta^{N-1}}{1 - \beta}\right)^{-1} \\ \lambda_2 = \beta_{12}\lambda_1 \\ \lambda_n = \beta^{n-2}\lambda_2, \quad 3 \leq n < N. \end{cases} \quad (23)$$

This eigenvalue spectrum idealizes the real examples to be shown in section 4.

The sample size (T) needed to obtain a desired expected correlation coefficient for the sample EOF1, and the true EOF1 can be estimated from (17) for any combination of λ_1 and β_{12} . In Fig. 2, results are shown for a hypothetical dataset with $N = 100$ eigenvalues and a threshold correlation coefficient of 0.975. The boundaries of the region reflect the fact that, for a given λ_1 , the possible range of β_{12} is constrained by the definition of the model.¹ For sufficiently large values of λ_1 (i.e., ≥ 0.6), for which λ_1 is necessarily well separated from

¹ For a given λ_1 , the lowest possible β_{12} occurs when $\beta = 1$. Then, from (23), $\beta_{12} = (1 - \lambda_1)/[\lambda_1(N - 1)]$. Also, from $\lambda_1 + \lambda_2 \leq 1$ and $\lambda_2 \leq \lambda_1$, it follows that the upper limit for β_{12} is $\min(1, 1 - \lambda_1/\lambda_1)$.

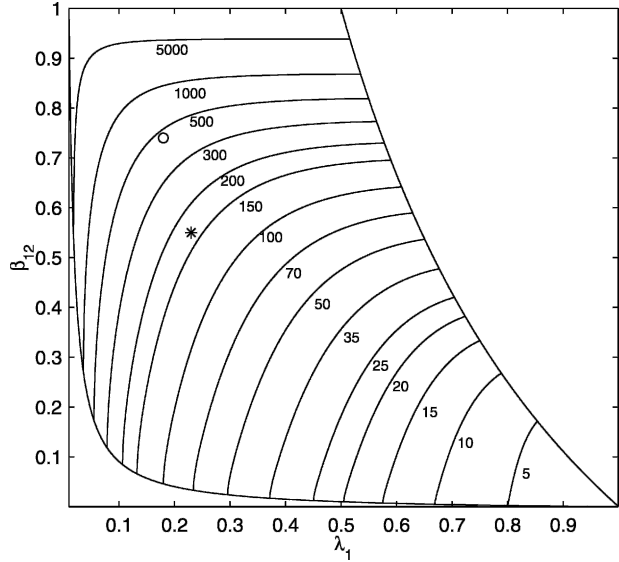


FIG. 2. Number of independent realizations in time (T) needed to expect a correlation coefficient of 0.975 between estimated and true leading EOF as a function of the values of λ_1 and $\beta_{12} = \lambda_2/\lambda_1$. Total number of eigenvalues: $N = 100$. The symbols (star and circle) indicate values of λ_1 and β_{12} corresponding to observations of SLP and 500 hPa, respectively (see section 4). See text for further explanation.

all other eigenvalues, mixing errors are small even for relatively small samples ($T \leq 100$). However, very large samples ($T > 500$) are needed to accurately estimate the first EOF when λ_2 is more than 80% of λ_1 ($\beta_{12} > 0.8$). In this case, β_{12} largely controls the necessary sample size T , except for very small values of λ_1 .

4. Sampling errors in geopotential height EOFs

Here we will use the results of section 2 to estimate the size of the sampling errors in the leading EOF of the Northern Hemisphere winter geopotential height field, at various levels. The dataset used is the National Centers for Environmental Prediction–National Centers for Atmospheric Research (NCEP–NCAR) reanalysis (Kalnay et al. 1996), obtained from the National Oceanic and Atmospheric Administration (NOAA) Climate Diagnostic Center (CDC). The data are gridded on a 2.5° latitude \times 2.5° longitude mesh. The fields used are sea level pressure (SLP) and 850-, 500-, 250-, 200-, 100-, 50-, 30-, and 10-hPa geopotential height. At each level, principal component analysis (PCA) is performed on the covariance matrix of monthly December–March (DJFM) anomalies for the period of record, 1958–99. The anomalies are area weighted by the square root of the cosine of latitude, and only the region north of 20°N is included in the analysis.

The sample size T is 168 months, but an effective sample size T^* for each level is computed by correcting T for the area-weighted lag-1 autocorrelation $\langle r \rangle$, according to the second-order formula given in Bretherton et al. (1999):

$$T^* = T \frac{(1 - \langle r \rangle^2)}{(1 + \langle r \rangle^2)}, \quad (24)$$

with typical values of $\langle r \rangle^2$ of ≈ 0.06 [$T^* \approx 150$, $\epsilon = (T^*)^{-1/2} \approx 0.08$] in the troposphere and ≈ 0.2 ($T^* \approx 110$, $\epsilon \approx 0.1$) in the stratosphere.

Figure 3 shows the observed eigenspectra of monthly mean SLP and 500-hPa geopotential height; in addition, it shows idealized fits to these spectra of the type analyzed in section 3. These fits are quite reasonable, showing that the idealized spectrum provides representative estimates of the sampling errors in the leading EOFs of our real datasets.

The first SLP EOF has been defined as the northern annular mode (Thompson and Wallace 1998), while the second is closely associated with the Pacific–North American pattern (Wallace and Thompson 2002; Quadrelli and Wallace 2004). These two modes are well separated from one another and from the third mode according to the criterion of North et al. (1982). At other tropospheric levels (e.g., 500 hPa; see Fig. 3), the two leading eigenvalues are generally less separated from one another than the leading SLP EOFs are.

Figure 4 shows expected mode mixing estimated from (11) for our specific example. The errors are expressed as angular standard deviations α_{ij}^* of the direction of the first sample EOF with its true direction, in the plane that it forms with each mixing EOF.

The leading EOF of SLP is expected to have smaller sampling errors than geopotential height at other tro-

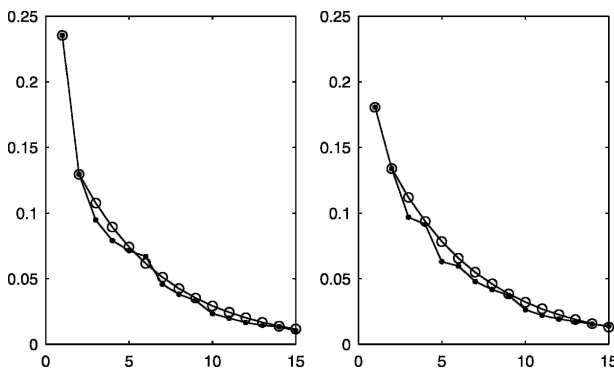


FIG. 3. Spectra of the eigenvalues normalized to a unit sum for (left) SLP and (right) 500-hPa geopotential height monthly mean fields (full circles), compared to a synthetic dataset with the same values of λ_1 and λ_2 , and constant ratio β between eigenvalues of higher order (empty circles). See text for further explanation.

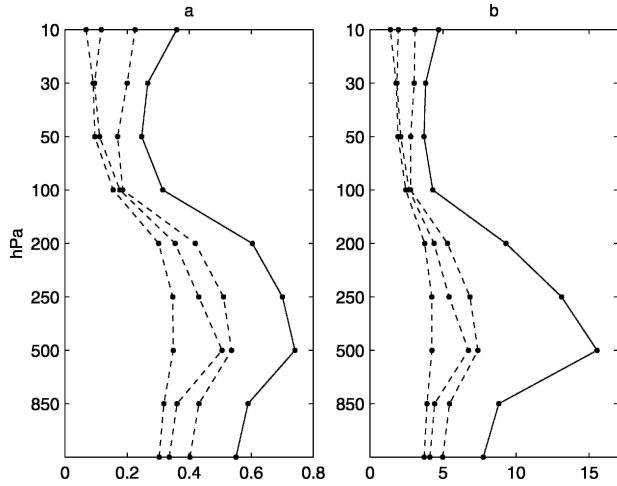


FIG. 4. Vertical profile of mixing errors in the leading EOF ($i = 1$): (a) ratio $\beta = \lambda_j/\lambda_1$ for $j = 2$ (solid) and $j = 3-5$ (dashed), and (b) angle α_{ij}^* ($^\circ$) between the sample and true EOF in the plane defined by the first and the j th EOFs, with $i = 1$, $j = 2$ (solid), and $j = 3-5$ (dashed). (a) and (b) are obtained using eigenvalues computed from the sample.

pospheric levels because its leading eigenvalue λ_1 is more dominant than in the midtroposphere (Fig. 3), so β_{ij} and α_{ij}^* are also correspondingly smaller. The SLP EOF1 angular standard deviation due to mixing between the leading two EOFs is estimated to be about 8° .

At all stratospheric levels, the sampling errors for the leading EOF are very small (2° – 5°), because the inherently low complexity of geopotential variability there makes the first eigenmode even more dominant than at the surface. The leading EOF at the 500-hPa level is subject to particularly high mixing errors with all the subsequent three modes and therefore is quite sensitive to sampling variability.

Figure 5 plots the expected cumulative effect of mode mixing with the first n EOFs on the correlation of the sample EOF1 ($i = 1$) and EOF2 ($i = 2$) with the respective true EOF,

$$r_n = 1 - 0.5 \sum_{1 < j \leq n} \alpha_{ij}^{*2}. \quad (25)$$

For EOF1 of both SLP and 500 hPa, mode mixing with the second eigenvector contributes roughly half, with EOFs 3–5 contributing another 25%. SLP EOFs 1 and 2 are much more robust with respect to sampling variability, compared to the respective EOFs of the 500-hPa level. The error in the leading 500-hPa EOF is in fact comparable to the error in EOF2 of SLP. The cumulative contributions of modes higher than 15 do not significantly alter the correlations shown for $n = 15$.

Figure 6 shows, for the two levels, two pairs of

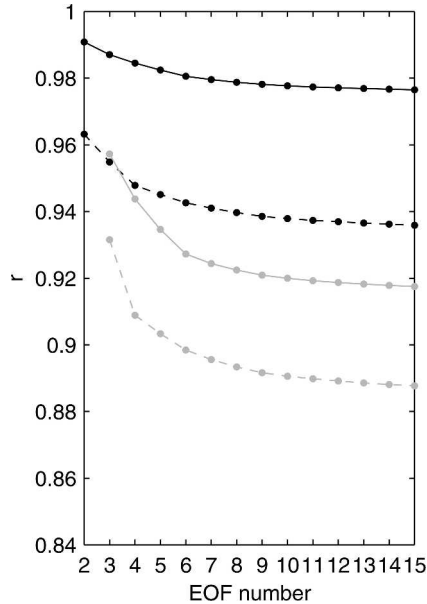


FIG. 5. SLP (solid) and 500-hPa (dashed) errors in EOF1 (and EOF2, in gray): expected correlation coefficient between sample and true EOF after cumulative mixing with EOFs up to 15. The error on EOF2 also includes the contribution from EOF1.

sample EOFs $\hat{\mathbf{e}}_1 = \mathbf{e}_1 + \sum_{j=2}^{15} \alpha_{1j}^* w_{1j} \mathbf{e}_j$, with $w_{1j} = +1$ for all j in the left panel and $w_{1j} = -1$ for all j in the right panel. These maps represent examples of the sampling variability that can be expected when computing EOFs from the current record of data.² At both levels, the strength of the Pacific center in the leading EOF is quite sensitive to sampling variability. However, over the Atlantic sector, the SLP EOFs are nearly identical, whereas the 500-hPa EOFs are quite different: one exhibits zonally elongated features and the other much is more wavelike. The area-weighted correlation coefficients between each perturbed map and the unperturbed EOF are 0.94 for 500 hPa and 0.98 for SLP, in agreement with the values shown in Fig. 5.

These empirical results are in agreement with the analysis of the hypothetical EOF spectrum presented in section 3. In the observed dataset, which consists of about 150 independent time realizations, the sizes of the errors are expected to be substantially different for SLP and 500 hPa. Based on the results of Fig. 2, it is estimated that in order to reduce the sampling error in the leading 500-hPa height EOF to that of the leading SLP EOF it would be necessary to triple the number of independent monthly samples from ~ 150 to ~ 450 .

² The EOF variability shown in Fig. 6 is typical, based on visual inspection of the sample EOFs that would be generated by (9) with 10 randomly chosen combinations of weights w_{1j} .

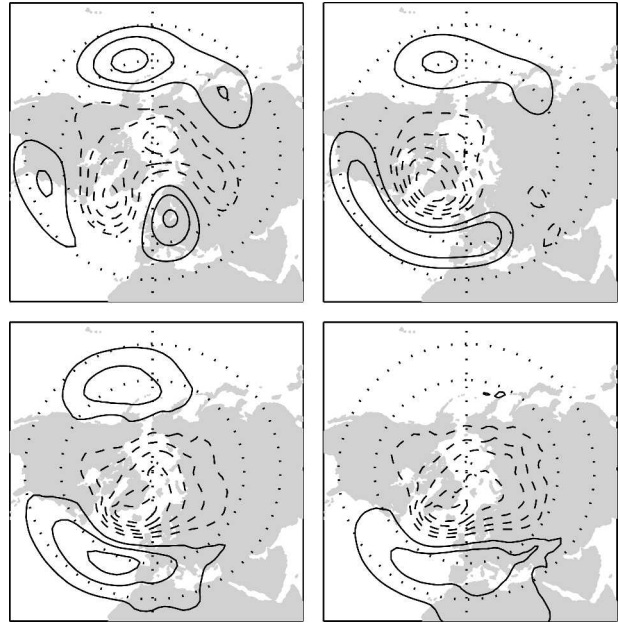


FIG. 6. Leading sample EOF of (top) 500-hPa geopotential height and (bottom) SLP including plus or minus one standard deviation contributions due to mode mixing with the respective EOFs 2–15 for a sample of size $T^* = 150$. Contour intervals: 15 m (500 hPa) and 1.2 hPa (SLP).

5. Conclusions

We have developed simple, easily applied formulas for estimating how reliably an EOF of a time-varying field of data can be determined from a finite data record. The formulas show that if the North et al. (1982) criterion holds for the corresponding eigenvalue of the covariance matrix, the EOF can be estimated fairly reliably. We use monthly mean Northern Hemisphere wintertime 500-hPa geopotential height and SLP as examples and find that the leading EOF of SLP can be estimated to within approximately half the error of the leading EOF of 500-hPa height from the current data record.

REFERENCES

- Bretherton, C. S., M. Widmann, V. P. Dymnikov, J. M. Wallace, and I. Bladé, 1999: The effective number of spatial degrees of freedom of a time-varying field. *J. Climate*, **12**, 1990–2009.
- Girshick, M. A., 1939: On the sampling theory of the roots of determinantal equations. *Ann. Math. Stat.*, **10**, 203–224.
- Jackson, J., 1991: *A User's Guide to Principal Components*. Wiley, 569 pp.
- Kalnay, E. M., and Coauthors, 1996: The NCEP/NCAR 40-Year Reanalysis Project. *Bull. Amer. Meteor. Soc.*, **77**, 437–471.
- Kim, K.-Y., 1996: Temporal and spatial subsampling errors for global empirical orthogonal functions: Applications to surface temperature field. *J. Geophys. Res.*, **101**, 23 433–23 446.
- North, G. R., T. L. Bell, R. F. Cahalan, and F. J. Moeng, 1982:

- Sampling errors in the estimation of empirical orthogonal functions. *Mon. Wea. Rev.*, **110**, 699–706.
- Quadrelli, R., and J. M. Wallace, 2004: A simplified linear framework for interpreting patterns of Northern Hemisphere wintertime climate variability. *J. Climate*, **17**, 3728–3744.
- Storch, H. V., and Hannoschöck, 1985: Statistical aspects of estimated principal vectors (EOFs) based on small sample sizes. *J. Climate Appl. Meteor.*, **24**, 716–724.
- Thompson, D. W. J., and J. M. Wallace, 1998: The Arctic Oscillation signature in the wintertime geopotential height and temperature fields. *Geophys. Res. Lett.*, **25**, 1297–1300.
- Wallace, J. M., and D. W. J. Thompson, 2002: The Pacific center of action of the Northern Hemisphere annular mode: Real or artifact? *J. Climate*, **15**, 1987–1991.
- Wilkinson, J., 1965: *The Algebraic Eigenvalue Problem*. Oxford University Press, 266 pp.